Development of a ConvLSTM-Net Model for Coastal Erosion Hazard Prediction Based on Spatiotemporal Data

Willy Boen
Computer Science Department, School of Computer Science, Bina Nusantara University, Indonesia
willy.boen@binus.ac.id (corresponding author)

Goldwin Hoxenlly
Computer Science Department, School of Computer Science, Bina Nusantara University, Indonesia
goldwin.hoxenlly@binus.ac.id

Ivander Hanson Setyawan
Computer Science Department, School of Computer Science, Bina Nusantara University, Indonesia
ivander.setyawan@binus.ac.id

Edy Irwansyah
Computer Science Department, School of Computer Science, Bina Nusantara University, Indonesia
edirwan@binus.ac.id

Vini Indriasari
Master of Computer Science Department, Binus Graduate Program, Bina Nusantara University, Indonesia
vini.indriasari@binus.ac.id

Received: 4 February 2026 | Revised: 15 March 2026 and 22 March 2026 | Accepted: 23 March 2026

 DOI: https://doi.org/10.48084/etasr.17951

ABSTRACT

Coastal erosion is a complex and dynamic process influenced by nonlinear interactions between spatial factors, such as shoreline geometry and land use, and temporal drivers including wave activity, sea-level rise, and climatic variability. Most previous research relies on deterministic or numerical models that, while physically interpretable, often lack adaptability and generalization across different coastal environments, whereas machine learning approaches are commonly limited to classification or factor analysis rather than direct spatiotemporal prediction. To address these limitations, this research proposes a Convolutional Long Short-Term Memory (ConvLSTM)-Net model to predict coastal erosion along the northern coast of Indramayu, West Java, Indonesia using the Landsat dataset. By integrating convolutional layers for spatial feature extraction with recurrent units for temporal dependency modeling, the proposed approach enables automated and scalable forecasting of shoreline evolution, offering a data-driven decision-support tool for coastal management and erosion mitigation in vulnerable coastal regions. The results show the ConvLSTM-Net model achieving a Dice score of around 99% and an Intersection over Union (IoU) of around 98%. These findings suggest that integrating convolutional and recurrent architectures effectively captures complex coastal transformations, providing a robust tool for long-term coastal management and disaster mitigation.

Keywords-coastal erosion; ConvLSTM; ConvLSTM-Net; LSTM; U-Net; prediction; spatiotemporal

I. INTRODUCTION

The phenomenon of coastal erosion in Indonesia continues to pose a serious threat to both human life and infrastructure. With more than 81,000 km of shoreline, Indonesia is one of the countries most vulnerable to coastal hazards in the world, driven by both natural processes, such as sea-level rise, as well as anthropogenic activities like sand mining [1, 2]. According to the coastal erosion disaster data recorded by the National Disaster Management Agency (BNPB) from 2000 to 2025, ten

people were reported dead, three went missing, and 196 suffered injuries. In addition, 4,349 houses were damaged, 4,022 were flooded, and 149 public facilities were affected [3].

Recent research has confirmed that several coastal regions, such as West Sumatra and the northern coast of Java, are undergoing significant shoreline retreat, with rates reaching up to 1.81 m per year in certain areas. These changes are driven by a combination of natural factors, such as sea-level rise and wave dynamics, as well as human-induced pressures like tourism development and land-use changes [4-6]. The spatial and temporal characteristics of erosion vary greatly across regions, making it a complex phenomenon to predict, especially in rapidly changing coastal environments. This growing complexity highlights the need for advanced computational approaches, particularly those based on Artificial Intelligence (AI), to analyze and forecast multi-dimensional geospatial data more accurately.

Advancements in AI have opened new possibilities for addressing this problem. In the field of geospatial science, machine learning techniques have been increasingly utilized to analyze both spatial and temporal datasets related to shoreline changes. However, traditional models often face critical limitations such as the inability to simultaneously process spatial and temporal features and the limited availability of high-quality datasets.

To overcome these challenges, deep learning approaches, especially Convolutional Long Short-Term Memory (ConvLSTM) networks, have emerged as promising alternatives. ConvLSTM combines the spatial feature extraction capabilities of Convolutional Neural Networks (CNNs) with the temporal sequence modeling strength of Long Short-Term Memory (LSTM) networks. Previous research [7] has demonstrated the success of ConvLSTM in various applications, such as rainfall prediction and environmental system dynamics [8, 9].

However, ConvLSTM alone often struggles with retaining fine-grained spatial details, especially in tasks requiring high-resolution segmentation, such as shoreline detection. To address this limitation, researchers have proposed integrating U-Net, a symmetric encoder–decoder network with skip connections that preserve spatial features during upsampling. The ConvLSTM-Net hybrid model combines the strengths of both: spatiotemporal sequence learning and precise spatial localization [10, 11].

Recent research has shown the effectiveness of ConvLSTM-Net in modeling complex hydrological dynamics and spatial changes. For instance, authors in [10] proposed a ConvLSTM-Net architecture for basin-scale hydrodynamic prediction, integrating remote sensing data with physical modeling. Similarly, authors in [11] proposed a ConvLSTM-Net model to forecast sea ice extent using multisource satellite time series data. Despite this progress, applications of this model in coastal erosion prediction remain limited, particularly in data-scarce regions such as Indonesia. Yet, this model has great potential to provide more accurate predictions by leveraging historical observational data of a spatiotemporal nature.

Therefore, the objective of this research is to develop a prediction model using ConvLSTM-Net based on spatiotemporal data to accurately predict coastal erosion hazards. This will be achieved by analyzing patterns and trends found in spatiotemporal data to provide information related to coastal erosion hazards and offer recommendations regarding the application of the model in real-world coastal erosion scenarios.

II. WORLDWIDE EXPERIENCES

This section discusses related research on coastal erosion, a phenomenon that has worsened due to the effects of climate change [12]. Coastal erosion results from complex interactions between spatial variables such as shoreline position, topography, and land use, and temporal factors including wave activity and seasonal weather patterns.

Most existing research relies on deterministic or numerical modeling approaches. Table I summarizes representative research from the past few years.

TABLE I. COMPARISON OF PREVIOUS RESEARCH ON COASTAL EROSION PREDICTION

Ref.	Research area	Dataset	Method
[2]	San Lorenzo Beach, Spain	Wave models, SLR (3 percentiles), 6 GCMs, 2 CEMs, VAR simulations	Top-down ensemble: CEM1 + CEM2 + climate VAR + SLR scenarios
[6]	Calabria, Italy	Historical shorelines (1954–2015), orthophotos, Google Earth	QGIS + index-based (NSM, EPR, CVI)
[12]	Maeng Bang Beach, Korea	Wave, river runoff, sediment, shoreline obs. (1971–2020)	IN-MPaS (one-line shoreline model + SWAT + sediment model)
[13]	Sicily, Italy	DEM (2m), CMEMS, WaTEM/SEDEM, ISPRA shoreline, 23,680 transects (2000–2020)	CeVI (index of 5 physical vars) + validation with shoreline shift
[14]	Saint Louis, Senegal	Pleiades DEM, Landsat, Sentinel-2, GPS transects, ERA5 wave data	DEM comparison, CoastSat shoreline tracking, stochastic spit growth model
[15]	Catania Plain, Italy	Landsat, Sentinel-2 (1972–2022), DSAS indices	DSAS + Kalman filter
[16]	Kenya	Landsat, NDVI, DEM, meteorology	RUSLE + GIS
[17]	Yzerfontein, South Africa	Aerial (1937–1977), Landsat (1985–2020), GEE, CoastSat	DSAS + CoastSat + WLR forecasting
[18]	Quang Ngai, Vietnam	Landsat, Sentinel, Aqua Monitor, MIKE21, LITPACK	Remote sensing + typhoon erosion modeling

Spatiotemporal remote sensing has been extensively used in coastal erosion research due to its capability to capture shoreline geometry and temporal changes over long observation periods. Landsat satellite imagery is widely adopted as the primary data source because of its long historical archive, consistent spatial resolution, and free global accessibility.

Previous research has employed multi-temporal Landsat data to extract shoreline positions and analyze erosion trends using statistical and numerical approaches, such as linear and

weighted linear regression implemented through the Digital Shoreline Analysis System (DSAS) [12, 17]. These approaches demonstrate the effectiveness of Landsat-based spatiotemporal analysis for long-term shoreline monitoring and erosion rate estimation.

Recent coastal research has increasingly adopted deep learning-based spatiotemporal models to address the limitations of traditional approaches. A hybrid model combining ConvLSTM and U-Net is particularly effective in modeling spatial patterns and temporal dependencies in remote sensing data. By integrating convolutional operations with an encoder–decoder structure, ConvLSTM-Net enables multi-scale spatial feature extraction while preserving temporal continuity across sequential satellite images, making it suitable for coastal erosion analysis.

In coastal applications, ConvLSTM-Net models have been used to learn shoreline evolution from multi-temporal satellite imagery. By processing image sequences as spatiotemporal inputs, the model captures non-linear coastal dynamics and supports pixel-level prediction, positioning ConvLSTM-Net as a promising framework for spatiotemporal coastal erosion prediction.

The research reviewed in Table I shows increasing sophistication in data usage, but most still lack automated pattern recognition or generalizable forecasting mechanisms. This is where AI, particularly deep learning models such as ConvLSTM, may offer significant advancements.

Some recent papers have explored machine learning in coastal engineering more broadly [19], but their application has mostly been limited to factor analysis or classification tasks, not spatiotemporal erosion prediction itself. Numerical methods and machine learning provide high accuracy in predicting coastal erosion. However, deep learning has not yet been widely utilized for this purpose.

Motivated by these gaps, this research proposes a ConvLSTM-Net model to predict coastal erosion. ConvLSTM-Net is a hybrid deep learning architecture that integrates ConvLSTM with an encoder–decoder convolutional network to extract spatial features from satellite imagery while capturing temporal dynamics across sequential observations. This architecture is particularly well suited for spatiotemporal data, enabling effective modeling of the evolution of coastal environments. The proposed model aims to provide adaptive, scalable, and automated predictions for vulnerable coastal zones by learning complex patterns from multi-year satellite imagery and environmental parameters.

III. METHODOLOGY

This section delineates the methodological framework utilized in this research. The methodology is illustrated in Figure 1, where each distinct color represents one of the four principal stages: data collection, data pre-processing, modeling, and evaluation. Initially, relevant data are collected, then pre-processed to ensure data quality, and then a prediction model is developed. The model is assessed by comparing it with actual observed data to determine performance.

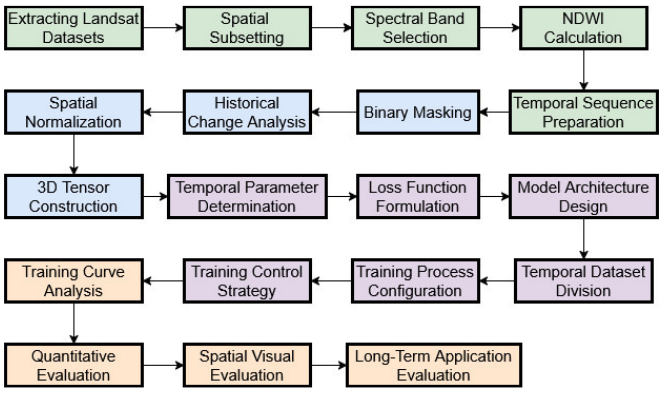

Fig. 1. Research workflow.

A. Data Collection

This research utilizes 36 annual Landsat images (1988–2023) obtained via the Google Earth Engine platform to analyze coastal dynamics in Indramayu, Indonesia (Figure 2). This dataset is part of the 50-year multispectral archive providing medium-resolution observations [20]. Each image was selected at the end of the year to ensure temporal consistency.

Fig. 2. Northern coastal area of Indramayu Regency, West Java, Indonesia derived from Landsat imagery accessed via Google Earth Engine [20].

All imagery in Table II was spatially subset using a polygon vector delineating the research area. All datasets are taken at the end of the year. Green and Near-Infrared (NIR) band data were also collected from each Landsat dataset to calculate the Normalized Difference Water Index (NDWI). Mathematically, NDWI is defined as follows [14]:

$$\text{NDWI} = \frac{Green_{band} - InfraRed_{band}}{Green_{band} + InfraRed_{band}} \quad (1)$$

TABLE II. DETAILS OF LANDSAT DATA

Landsat data	Sensor	Spatial resolution	Green band	NIR band
1-3	Multispectral Scanner (MSS)	60 m	B4	B6
4			B1	B3
5	Thematic Mapper (TM)	30 m	SR_B2	SR_B4
7	Enhanced Thematic Mapper Plus (ETM+)			
8	Operational Land Imager (OLI)		SR_B3	SR_B5
9	OLI-2			

The resulting NDWI images were organized as a temporal sequence covering the period from 1988 to 2023 and stored in raster format. Historical limitations in data acquisition and distribution resulted in incomplete data availability for certain periods, which is reflected in the temporal coverage of the dataset. Therefore, the continuous temporal analysis primarily covers the period from 1988 to 2023, which corresponds to the operational period of Landsat 5.

B. Data Pre-Processing

After obtaining the NDWI in raster form, binary masking is performed to identify land and water. The masking is done by applying a thresholding operation using a zero-threshold value. Mathematically, each pixel is classified as either water or land, so the binary masking is defined as follows:

$$Mask(x,y) = \begin{cases} 1, & \text{NDWI}(x,y) > 0 \implies \text{Water} \\ 0, & \text{NDWI}(x,y) \leq 0 \implies \text{Land} \end{cases} \quad (2)$$

The resulting classification mask is stored in raster format for each specified year. Then, the identification of coastline changes was carried out by intersecting the coastline in 1988 with that of 2023. This process was carried out to compare the distribution of water and land pixels in the two periods, so that a natural pattern of changes in the coastline of the north coast of Indramayu was obtained.

After that, the annual shoreline binary masks are sorted temporally by year, which are then resized to a uniform spatial dimension of 512 × 512 pixels. This is performed using nearest neighbour interpolation to maintain their discrete class values.

Next, all data are arranged into a time series in the form of a three-dimensional tensor with dimensions $N \times H \times W$, where N is the number of images used, whereas H and W indicate the height and width of the image. This process produces spatiotemporal consistency.

After that, the data are standardized using a z-score and divided into input–output sequences using a sliding window approach to capture the model's temporal dependencies. Each iteration, as many as T consecutive annual images are used as input for the next year's image prediction. This process makes each input sample have dimensions of $T \times H \times W$. Meanwhile, the target output is represented in the form of dimensions $H \times W$, thus producing data pairs (x, y) that can capture inter-annual spatiotemporal dynamics and are suitable for model training.

C. Modeling

After data pre-processing and before model training begins, the temporal window length was set at $T = 3$, with a dropout rate of 0.1. This process was performed to reduce the risk of overfitting. The training process was controlled by an early stopping scheme based on the validation loss value, which aims to stop training when there is no significant performance improvement.

This research employs a mixture of Binary Cross-Entropy (BCE) and Dice loss [21], along with Tversky loss, to mitigate class imbalance in coastal segmentation, effectively regulating the penalty between false positives and false negatives during training. This loss function facilitated the model's acquisition of a more equitable and consistent spatial representation for forecasting coastal topologies in future temporal intervals.

The proposed architecture in Figure 3 adopts the concept of spatiotemporal modeling by integrating spatial feature extraction and temporal dependency modeling capabilities. Specifically, the temporal modeling component of this architecture is realized using ConvLSTM, which is designed to handle time series data in the form of images while preserving its spatial structure. The ConvLSTM formulation used refers to the approach introduced by authors in [22], who extended the conventional LSTM by replacing the matrix multiplication operation with a convolution operation.

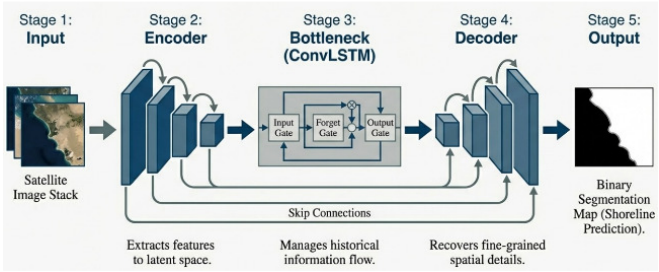

Fig. 3. ConvLSTM and U-Net architecture.

Mathematically, the ConvLSTM at each time step is refined as follows [22]:

$$i_t = \sigma(W_{xi} * X_t + W_{hi} * H_{t-1} + W_{ci} \circ C_{t-1} + b_i) \quad (3)$$

$$f_t = \sigma\big(W_{xf} * X_t + W_{hf} * H_{t-1} + W_{cf} \circ C_{t-1} + b_f\big) \quad (4)$$

$$C_t = f_t \circ C_{t-1} + i_t \circ \tanh(W_{xc} * \mathcal{X}_t + W_{hc} * H_{t-1} + b_c) \quad (5)$$

$$o_t = \sigma(W_{xo} * X_t + W_{ho} * H_{t-1} + W_{co} \circ C_t + b_o) \quad (6)$$

$$H_t = o_t \circ \tanh(C_t) \quad (7)$$

This formulation shows that each time step t begins with the calculation of an input gate (i_t), a forget gate (f_t), and an output gate (o_t), which function to regulate the flow of information into, retain, or release information from the cell's memory (C_t) with weight control (W) and bias (b). The input gate determines the extent to which new information from the spatial input (X_t) will be updated into memory, whereas the forget gate controls the proportion of historical information from the previous cell state that is retained. The output gate determines the portion of memory information that will be projected as the hidden state (H_t).

Within the U-Net architecture, spatial characteristics are sequentially extracted throughout the encoding process and subsequently mapped onto a latent space. The ConvLSTM model processes this latent representation at the bottleneck to capture temporal dependencies and spatiotemporal dynamics. The decoder subsequently reconstructs spatial predictions using upsampling and convolution, employing skip connections from the encoder to retain critical spatial features. The network's ultimate output is a predicted shoreline configuration

represented as a binary segmentation map that depicts the expected shoreline configuration for the upcoming period.

After creating classes for early stopping and loss calculations, and defining the model architecture, the data are divided into training data, validation data, and test data. The data are divided temporally with ratios of 80% (1988–2017), 10% (2018–2020), and 10% (2021–2023). This division is done based on chronological order for continuous prediction, with the oldest data used for training, followed by the validation data, and then the test data. This approach is taken to ensure a sequential historical scenario of real conditions that will be used for future predictions.

After that, the training and validation data are then converted into tensors and arranged in dimensions (B, T, C, H, W), which represent the batch size (B), temporal window length (T), number of channels (C), and spatial dimensions of the image (H, W). The ConvLSTM-Net model is trained using the AdamW optimizer with an initial learning rate of 2×10^{-4} and with a weight decay of 1×10^{-5}. The model is then trained with a loss function to handle class imbalance.

Meanwhile, the learning rate is adjusted using the ReduceLROnPlateau scheme based on the validation loss value. The training process is also controlled by an early stopping mechanism to stop training when no significant performance improvement is observed.

The model was trained in an iterative manner under a supervised learning framework. Each iteration, the model is trained with training data, minimizing the loss function using the AdamW optimization algorithm. During training, the gradient is calculated using backpropagation, and the model parameters are gradually updated. Model performance is monitored using validation data, which calculates the adjusted validation loss using the learning rate adjustment. This approach is expected to achieve stable training and ensure the model reaches optimal convergence before being used in the final evaluation stage.

D. Evaluation

During the training process, the model is evaluated using the training and validation loss values at each epoch and visualized as a curve to assess the model's stability. The test data are evaluated using the Dice Coefficient and Intersection over Union (IoU) metrics. Mathematically, both Dice and IoU are defined as follows [23]:

$$\text{IoU} = \frac{|Predicted\ Mask \cap Ground\ Truth\ Mask|}{|Predicted\ Mask \cup Ground\ Truth\ Mask|} \quad (8)$$

$$\text{Dice} = \frac{2\ x\ |Predicted\ Mask \cap Ground\ Truth\ Mask|}{|Predicted\ Mask| + |Ground\ Truth\ Mask|} \quad (9)$$

These metrics evaluate the degree of geographical alignment between the model's predictions and its reference mask. The Dice coefficient emphasizes overall agreement, whereas the IoU measures the overlap between the predicted area and the actual data. This evaluation was performed on the entire test dataset to ascertain the model's overall effectiveness.

A visual assessment was conducted alongside the numerical analysis by juxtaposing the projected outcomes with the actual mask in the test data. This analysis illustrates accurately anticipated regions against inaccurately expected areas. This seeks to elucidate the error patterns in the evaluation, specifically concerning the shoreline transition zone. This method offers a spatial analysis of prediction errors inadequately represented in the numerical assessment.

The model's prediction results analyze long-term shoreline changes by comparing the initial and final conditions of the observation period as an application-based evaluation. The extent of abrasion and accretion is calculated by measuring the change in pixel status between the two observation times, both in actual data and prediction results. This analysis illustrates the model's ability to represent shoreline change dynamics quantitatively and spatially, supporting research objectives in the context of predicting shoreline change.

IV. RESULTS AND DISCUSSION

This section discusses the changes in the original north coastline of Indramayu from 1988 to 2023. In addition, this section presents the model validation results, the determination of the optimal threshold, the model testing results, and the continuous prediction results derived from the training data (1988–2017) and applied to the prediction period (2018–2023).

The actual shoreline changes from 1988 to 2023, as shown in Figure 4, provide an analysis of the magnitude of the changes that occurred, where the black color represents the water mask and the remaining areas represent land. The panel shows 1988 and 2023. These are then combined to provide an analysis of the shoreline changes that occurred. The red and green areas show changes in the condition of the northern coastline of Indramayu.

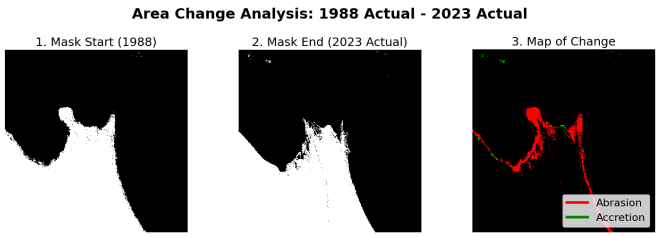

Fig. 4. Shoreline change dynamics in the northern coast of Indramayu Regency, West Java, Indonesia from 1988 to 2023.

Figure 4 shows that most areas experienced abrasion rather than accretion. The total shoreline change was 8,930 pixels, where each pixel represents 30 m; therefore, the average distance of change was 267,900 m. The total area of change is 8,037,000 m², indicating substantial spatial transformation along the coastline. These results further highlight the presence of significant coastal dynamics during the observation period.

The training and validation loss curves in Figure 5 demonstrate the ConvLSTM-Net model's effectiveness, characterized by a sharp initial decrease followed by stable convergence. These patterns indicate a rapid learning rate process and strong generalization capability, with no clear signs of significant overfitting. Although the stability of the final validation loss suggests that the model has achieved near-

optimal convergence, comprehensive testing is still required to fully validate the model's performance and ensure its reliability before deployment.

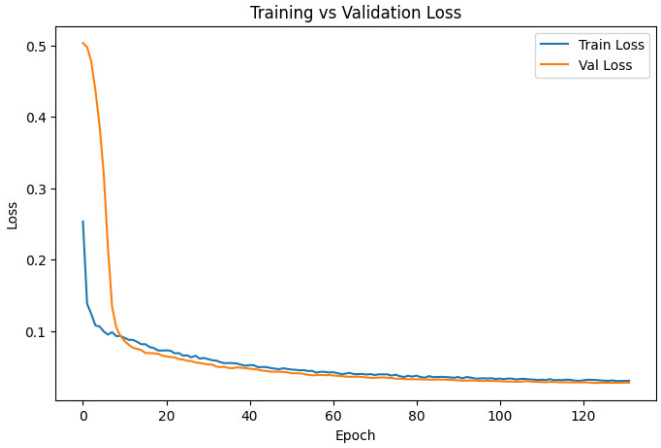

Fig. 5. Training and validation loss.

A comparison of the model's prediction results with the test data is shown in Figure 6. The results again prove that the model is highly effective. The Dice score is around 99%, and the IoU score is around 98%. The predicted errors shown in the three figures are very small, although the errors are still above 1,000 pixels. However, the correct predictions are more dominant than the prediction errors, so the model is still considered usable. This proves that the model is able to represent the predicted configuration of the coastline each year, although there are still local errors around the complex coastline transition zone.

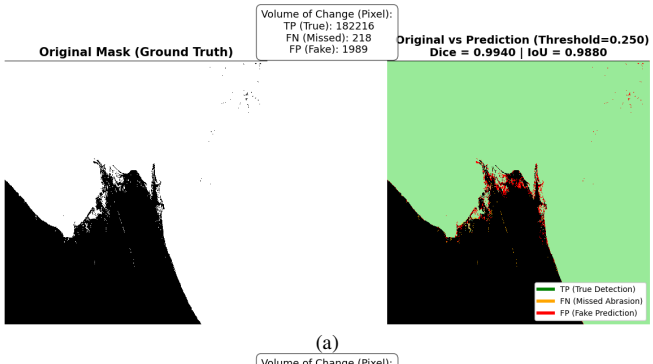

(a)

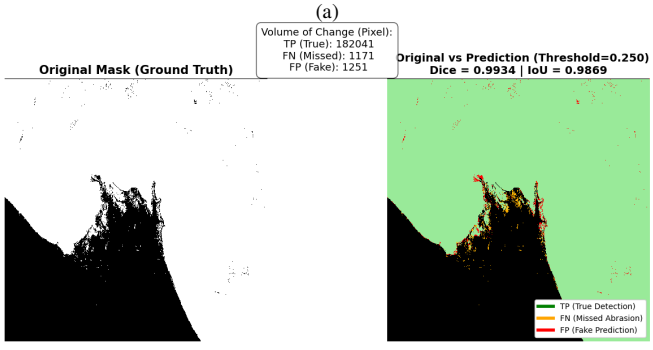

(b)

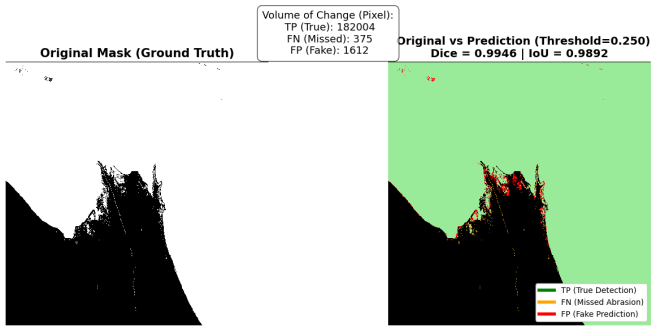

(c)

Fig. 6. Comparison of the ground truth and predicted shoreline masks: (a) 2021, (b) 2022, (c) 2023.

The threshold optimization shown in Figure 7 is used to convert the probabilistic outputs of the model into binary segmentation masks. This evaluation is conducted using the validation data by computing the mean Dice score across a range of threshold values. The results indicate that a threshold value of 0.25 yields the highest Dice score and is therefore selected as the optimal threshold for the inference stage.

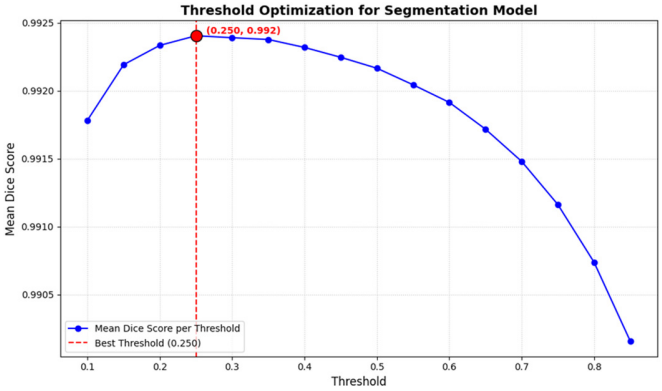

Fig. 7. Threshold optimization for the segmentation model.

The shape of the curve demonstrates that excessively high threshold values tend to reduce segmentation performance, reflecting a trade-off between sensitivity and specificity in pixel-level classification. Selecting this optimal threshold ensures that the predicted results used in subsequent evaluation and analysis achieve the highest possible spatial agreement with the reference data. The shoreline changes analysis reveals significant coastal dynamics during the observation period, with Figure 4 showing a total change of 8,930 pixels, equivalent to an average distance of 267,900 m and a total area of 8,037,000 m², where abrasion predominantly exceeds accretion. These actual observations, derived from the 1988–2017 training period, serve as the baseline for the model to predict the remaining.

The resulting analysis in Figure 8 shows that the difference between the actual 2023 configuration and the model's prediction is only 921 pixels, or 828,900 m². This minimal discrepancy confirms that the ConvLSTM-Net model is highly successful in predicting the long-term evolution of Indramayu's northern coastline with a very small margin of error.

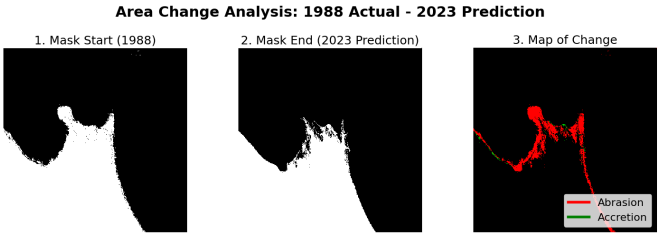

Fig. 8. Shoreline changes predicted by the model.

Beyond quantitative differences, the agreement between the predicted spatial patterns of abrasion and actual data demonstrates the model's ability to capture the main dynamics of shoreline change in the research area. Model prediction errors, particularly in coastal transition zones with high morphological complexity, such as estuaries and shallow waters, are inherently difficult to distinguish clearly using medium-resolution data. This suggests that the errors are local and not systemic.

Overall, the quantitative and visual evaluation results demonstrate that the ConvLSTM-Net model is capable of effectively capturing the spatiotemporal dynamics of shoreline change with a high level of agreement. The prediction errors observed are limited and spatially localized, primarily occurring in areas with high morphological complexity. Furthermore, the comparison between Figures 4 and 8 confirms the ability of the ConvLSTM-Net model to reliably predict shoreline configurations over long-term temporal intervals.

However, this research still suffers from limitations in the spatial resolution of Landsat data and spectral index ambiguity in certain areas, which are factors that affect prediction accuracy. These findings demonstrate that the ConvLSTM-Net approach has strong potential for application in predicting coastal changes through satellite imagery. Furthermore, these findings also indicate the dominance of significant abrasion in certain segments, necessitating further policy measures to prevent abrasion disasters.

V. CONCLUSION

This study demonstrates that the Convolutional Long Short-Term Memory (ConvLSTM)-Net architecture is highly effective for predicting spatiotemporal changes along the northern coast of Indramayu, West Java, Indonesia. The results indicate that the proposed model successfully captures long-term coastal dynamics, achieving a Dice score of approximately 99% and an Intersection over Union (IoU) of 98%. Visually and quantitatively, the model produced stable and consistent predictions, replicating major patterns of abrasion and accretion with high agreement against actual data. Minor errors were localized primarily in morphologically complex areas, such as estuaries, suggesting that the model maintains high reliability across the majority of the study area.

From a methodological standpoint, integrating U-Net for multi-scale spatial feature extraction with ConvLSTM for temporal dependency modeling proves robust for medium-resolution satellite imagery. This combination allows for deep spatiotemporal learning without compromising the underlying spatial structure of the coastline. Practically, this approach serves as a viable supporting tool for coastal monitoring and risk analysis. By leveraging public satellite imagery, the model can contribute to periodic mapping, coastal development planning, and sustainable resource management, offering both methodological and applied contributions to the field.

Despite these positive outcomes, the research is constrained by the spatial resolution of Landsat data and the reliance on a single spectral index, which may introduce ambiguity in complex regions. Furthermore, external oceanographic factors such as tides and wave energy were not explicitly modeled. Future research should focus on integrating multi-source environmental data and implementing multi-step prediction schemes. Testing the model across diverse geomorphological coastal regions will be essential to verify its generalizability and further improve its utility for global coastal conservation efforts.

DECLARATION OF COMPETING INTERESTS

The authors declare that they have no competing interests.

ACKNOWLEDGMENT

The authors would like to thank the Binus Graduate Program and the School of Computer Science for facilitating this research and providing the necessary environment for its completion. This research received no specific grant from any funding agency in the public, commercial, or not-for-profit sectors.

DATA AVAILBILITY

The Landsat dataset used in this research was accessed through the Google Earth Engine platform. Detailed information regarding the dataset's integration within this cloud-based environment and its technical specifications follows the standards documented in [20]. Access link: https://developers.google.com/earth-engine/datasets/catalog/landsat.

AI USE AND DECLARATION OF GENERATIVE AI USE

During the preparation of this work, the authors used ChatGPT and Gemini for translating paragraphs from the Indonesian language into English, Quillbot for checking spelling and grammar, and NotebookLM for generating images for the methodology's model architecture. After using these tools, the authors reviewed and edited the content as needed and take full responsibility for the content of the publication.

REFERENCES

[1] D. N. Handiani, A. Heriati, and F. Suciaty, "Coastal Vulnerability Assessment Along The North Java Coastlines-Indonesia," *Jurnal Segara*, vol. 18, no. 1, pp. 1–12, Apr. 2022, https://doi.org/10.15578/segara.v18i1.10664.

[2] A. Toimil, P. Camus, I. J. Losada, and M. Alvarez-Cuesta, "Visualising the Uncertainty Cascade in Multi-Ensemble Probabilistic Coastal Erosion Projections," *Frontiers in Marine Science*, vol. 8, June 2021, Art. no. 683535, https://doi.org/10.3389/fmars.2021.683535.

[3] "Geoportal Data Bencana Indonesia." Badan Nasional Penanggulangan Bencana (BNPB). https://gis.bnpb.go.id/.

[4] A. W. Hastuti, M. Nagai, N. P. Ismail, B. Priyono, K. I. Suniada, and A. Wijaya, "Spatiotemporal analysis of shoreline change trends and adaptation in Bali Province, Indonesia," *Regional Studies in Marine*

Science, vol. 76, Dec. 2024, Art. no. 103598, https://doi.org/10.1016/j.rsma.2024.103598.

[5] P. M. Fairuzia, R. Rifardi, and S. H. Siregar, "Analysis of Shoreline Changes in the Coastal Area Between Batang Anai Estuary and Batang Mangur Estuary West Sumatra Province," *Journal of Coastal and Ocean Sciences*, vol. 4, no. 3, pp. 149–159, Sept. 2023.

[6] G. Foti, G. C. Barillà, G. Barbaro, and P. Puntorieri, "Remote Sensing And Gis To Support Coastal Erosion Risk Analysis In Calabria, Italy," *WIT Transactions on Engineering Sciences*, vol. 129, pp. 67–76, https://doi.org/10.2495/RISK200061.

[7] J. Yang, T. Zhang, J. Zhang, X. Lin, H. Wang, and T. Feng, "A ConvLSTM nearshore water level prediction model with integrated attention mechanism," *Frontiers in Marine Science*, vol. 11, Oct. 2024, Art. no. 1470320, https://doi.org/10.3389/fmars.2024.1470320.

[8] E. Gomez-de la Peña, G. Coco, C. Whittaker, and J. Montaño, "On the use of convolutional deep learning to predict shoreline change," *Earth Surface Dynamics*, vol. 11, no. 6, pp. 1145–1160, Nov. 2023, https://doi.org/10.5194/esurf-11-1145-2023.

[9] R. Yuan *et al.*, "Detecting Shoreline Changes on the Beaches of Hainan Island (China) for the Period 2013–2023 Using Multi-Source Data," *Water*, vol. 16, no. 7, Apr. 2024, Art. no. 1034, https://doi.org/10.3390/w16071034.

[10] A. Li *et al.*, "A Deep U-Net-ConvLSTM Framework with Hydrodynamic Model for Basin-Scale Hydrodynamic Prediction," *Water*, vol. 16, no. 5, Feb. 2024, Art. no. 625, https://doi.org/10.3390/w16050625.

[11] J. Park, Y. Cho, J.-J. Jeon, J. Park, H.-C. Kim, and S. Hong, "Unicorn: U-Net for sea ice forecasting with convolutional neural ordinary differential equations," *Scientific Reports*, vol. 15, no. 1, Oct. 2025, Art. no. 36330, https://doi.org/10.1038/s41598-025-20097-4.

[12] Y.-J. Kim and J.-S. Yoon, "Prediction of Shoreline Change for the Calculation of the Integrated Littoral Sediment Budget," *Water*, vol. 14, no. 2, Jan. 2022, Art. no. 232, https://doi.org/10.3390/w14020232.

[13] G. Manno *et al.*, "An Approach for the Validation of a Coastal Erosion Vulnerability Index: An Application in Sicily," *Journal of Marine Science and Engineering*, vol. 11, no. 1, Dec. 2022, Art. no. 23, https://doi.org/10.3390/jmse11010023.

[14] A. Taveneau *et al.*, "Observing and Predicting Coastal Erosion at the Langue de Barbarie Sand Spit around Saint Louis (Senegal, West Africa) through Satellite-Derived Digital Elevation Model and Shoreline," *Remote Sensing*, vol. 13, no. 13, June 2021, Art. no. 2454, https://doi.org/10.3390/rs13132454.

[15] F. A. T. Laksono, L. Borzì, S. Distefano, A. D. Stefano, and J. Kovács, "Shoreline Prediction Modelling as a Base Tool for Coastal Management: The Catania Plain Case Study (Italy)," *Journal of Marine Science and Engineering*, vol. 10, no. 12, Dec. 2022, Art. no. 1988, https://doi.org/10.3390/jmse10121988.

[16] Y. Hategekimana, M. Allam, Q. Meng, Y. Nie, and E. Mohamed, "Quantification of Soil Losses along the Coastal Protected Areas in Kenya," *Land*, vol. 9, no. 5, May 2020, Art. no. 137, https://doi.org/10.3390/land9050137.

[17] J. Murray, E. Adam, S. Woodborne, D. Miller, S. Xulu, and M. Evans, "Monitoring Shoreline Changes along the Southwestern Coast of South Africa from 1937 to 2020 Using Varied Remote Sensing Data and Approaches," *Remote Sensing*, vol. 15, no. 2, Jan. 2023, Art. no. 317, https://doi.org/10.3390/rs15020317.

[18] M. Sokolewicz, L. Bergsma, L. Schemmekes, H. Nguyen, and S. Boersen, "Use of Remote Sensing Techniques and Numerical Modelling to Predict Coastal Erosion in Vietnam," *Coastal Engineering Proceedings*, no. 36v, Dec. 2020, Art. no. papers.65, https://doi.org/10.9753/icce.v36v.papers.65.

[19] A. K. Saydjari, S. K. N. Portillo, Z. Slepian, S. Kahraman, B. Burkhart, and D. P. Finkbeiner, "Classification of Magnetohydrodynamic Simulations Using Wavelet Scattering Transforms," *The Astrophysical Journal*, vol. 910, no. 2, Apr. 2021, Art. no. 122, https://doi.org/10.3847/1538-4357/abe46d.

[20] M. A. Wulder *et al.*, "Fifty years of Landsat science and impacts," *Remote Sensing of Environment*, vol. 280, Oct. 2022, Art. no. 113195, https://doi.org/10.1016/j.rse.2022.113195.

[21] E. Irwansyah, A. A. S. Gunawan, H. Pranoto, F. S. Pramudya, and L. Fakhriadi, "Deep Learning with Semantic Segmentation Approach for Building Rooftop Mapping in Urban Irregular Housing Complexes," *Engineering, Technology & Applied Science Research*, vol. 15, no. 2, pp. 20580–20587, Apr. 2025, https://doi.org/10.48084/etasr.9670.

[22] X. Shi, Z. Chen, H. Wang, D.-Y. Yeung, W. Wong, and W. Woo, "Convolutional LSTM Network: A Machine Learning Approach for Precipitation Nowcasting," in *Proceedings of the 28th International Conference on Neural Information Processing Systems*, Montreal, Canada, 2015, pp. 802–810.

[23] I. Abbas, R. Damaševičius, R. Maskeliūnas, and M. A. Sarwar, "Tree Segmentation from Low-Resolution Digital Orthophotos using a Hybrid Deep Learning Model," in *Communication Papers of the 20th Conference on Computer Science and Intelligence Systems*, Kraków, Poland, 2025, pp. 1–8.